PAPER SUBMITTED TO *MATERIALS AND STRUCTURES / MATÉRIAUX ET CONSTRUCTIONS*
Reference number assigned by RILEM: MS

Right side of the page

Dynamic Pressurization Method for Measuring Permeability and Modulus: II. Cementitious Materials

Dynamic Pressurization Method for Measuring Permeability and Modulus: II. Cementitious Materials
Authors: Z.C. Grasley[1], G.W. Scherer[2*], D.A. Lange[1], J.J. Valenza[2]

(*) E319 Engineering Quad, Princeton University, Princeton, NJ 08544, USA
+1.609.258.5680
scherer@princeton.edu
(1) University of Illinois at Urbana-Champaign USA
(2) Princeton University USA

ABSTRACT

In a companion paper, the theory behind a novel method for measuring permeability and bulk modulus is derived. The new method is termed 'dynamic pressurization'. In this paper, an apparatus for the new method is described, and the test procedure is applied to cement pastes and concretes. The test involves rapidly applying a hydrostatic pressure to a saturated cylinder, then measuring the time-dependent deformation response of the material. The test is found to be repeatable, and the fitting function described in the companion paper is found to adequately fit the measured data. The measured permeability of the cement pastes compare well to measured values on identical materials using a different technique. The measured bulk moduli of the solid nanostructure of the cement pastes and concretes obtained in the dynamic pressurization test are in the range of expected values based on literature values for the Young's moduli of clinker and hydration products.

1. INTRODUCTION

Virtually all degradation mechanisms present in concrete pavements and structures are dependent on the movement of moisture and ions in the pore network. While diffusion, osmosis, and adsorption all play a role in this transport, permeability is the parameter most often chosen to represent concrete durability or quality. As permeability relates the ease with which a fluid may flow through a porous body based on a pressure differential, many experiments have been designed which directly measure the phenomena. A specimen is sealed around the perimeter, and a head of water pressure is applied to one face. The flowrate of water through the opposite face of the specimen is measured to quantify permeability. Examples of these type of systems include those designed by Hearn and Mills [1], Sosoro et al. [2], Mindess [3], Ye [4], and Hooton [5].

Right side of the page
reserved to our referees

These conventional techniques for measuring the permeability of cement paste or concrete have many potential shortcomings. Long test durations (often weeks) require some consideration of material aging and eliminate the possibility of measuring the evolution of permeability from young ages. It has been reported that for a 0.4 *w/c* paste, the permeability changes 6 orders of magnitude from the fresh state until 24 days [6]. The high pressures required to develop and maintain a constant flow rate through the specimen often initiate leaks through seals, resulting in exaggerated permeability coefficients. Clogging of pores may also be an issue. A large variability in test data may be a consequence of these limitations [7].

A non-traditional approach to quantifying permeability would involve measuring another time-dependent parameter that is dependent on the flow of a fluid within the porous material. For example, the short-term time-dependent deformation of saturated cementitious materials under load can be associated with the flow of capillary pore fluid from high compressive stress states to lower stress states. This was recognized by Sellevold et al. [8], who noted the rate of short-term creep was related to the viscosity of the pore fluid. More recently this phenomenon has been utilized to measure the permeability of cementitious materials through novel test procedures including thermopermeametry (TPA) [9]-[11], and beam bending (BB) techniques [12]-[15].

The TPA method involves measuring the thermal dilation kinetics of a saturated specimen. The rate of relaxation after initial dilation is dependent on the permeability and viscoelastic properties of the material. The BB method involves measuring the load necessary to maintain a constant deflection of a saturated beam. The measured load relaxation is dependent on the permeability and viscoelastic properties of the material. Both techniques involve creating a differential state of stress in the pore fluid that results in flow. Limitations of these techniques include large specimen size requirement for concrete, and viscoelastic deformation that seriously complicates the analysis of the results.

This paper describes the experimental procedure and apparatus for a new method for measuring the permeability of a porous material, along with the bulk modulus of the solid nanostructure. The theory behind the new method is described in a companion paper [20]. The experimental technique is based on the dynamic pressurization (DP) approach to measuring permeability utilized by Gross and Scherer [21] for determining the permeability of aerogels. Like TPA and BB, DP entails creating a differential state of stress in the pore fluid that results in flow. By measuring the deformation kinetics, the permeability may be ascertained. The final strain after pressurization is related to K_s.

The bulk modulus of the solid nanostructure, K_s, of cementitious materials may be quite useful in modeling bulk material response due to microscale stresses. For example, early drying shrinkage and self-desiccation shrinkage are believed to occur primarily as a result of changes in pore fluid pressure associated with the formation of capillary menisci [16]. Underpressure (analogous to tension) in the

pore fluid is balanced by corresponding compression in the solid nanostructure [17]. Models incorporating the elastic bulk modulus of the solid nanostructure have been developed for modeling deformations associated with pore fluid pressure [18]-[19]. However, due to the difficulty of experimentally obtaining *Ks*, application of these models has involved approximating the actual value.

2. THEORY

The DP technique involves rapidly applying a hydrostatic pressure on a saturated cylinder. The specimen is initially compressed volumetrically, then gradually re-expands to a final strain that is dependent on K_s. The re-expansion is caused by the flow of water from the high external pressure towards the center of the specimen where there is a lower internal pore fluid pressure. The rate of re-expansion is dependent on the rate of flow and thus the permeability of the specimen. When the external pressure is rapidly released, the specimen initially re-expands beyond the original volume, then gradually contracts back to zero strain. The rate of contraction is also dependent on the specimen permeability. A brief overview of the theory behind the DP experiment and analysis is included below. For a complete discussion, see the companion paper [20].

Based on Biot's constitutive relations [22], in the elastic case, the axial strain of a cylindrical sample following a step change in pressure is given by

$$\frac{\varepsilon_z(\theta)-\varepsilon_\infty}{\varepsilon_0-\varepsilon_\infty}=\Omega(\theta) \tag{1}$$

where the initial strain is

$$\varepsilon_0=-\frac{p_A}{3K_p}(1-b\,\lambda) \tag{2}$$

and the final strain is

$$\varepsilon_\infty=\frac{(b-1)\,p_A}{3K_p}=-\frac{p_A}{3K_S} \tag{3}$$

Here, K_p is the bulk modulus of the drained porous solid, $b=1-K_p/K_s$ is the Biot coefficient, $\lambda=Mb/(Mb^2+K_p)$, and M is the Biot modulus,

$$\frac{1}{M}=\frac{\phi}{K_L}+\frac{b-\phi}{K_S} \tag{4}$$

where ϕ is the porosity, and K_L is the bulk modulus of the pore fluid. The reduced time is $\theta=t/\tau_v$ and the hydrodynamic relaxation time, τ_v, is defined by

$$\tau_v=\frac{\eta_L\,R^2}{k}\left(\frac{\beta\,b^2}{K_p}+\frac{\phi}{K_L}+\frac{b-\phi}{K_S}\right) \tag{5}$$

where η_L is the viscosity of the pore liquid, R is the specimen radius, $\beta = (1+\upsilon_p)/(3-3\upsilon_p)$ where υ_p is the bulk modulus of the porous body, and k is the permeability of the porous solid in units of length squared. The flow is assumed to be governed by Darcy's Law, which states that the flux, J, is proportional to the gradient of the pressure, p, such that

$$J = -\frac{k}{\eta_L}\nabla p \qquad (6)$$

The exact relaxation function is complicated, but is very accurately represented by

$$\Omega(\theta) \approx \exp\left\{\frac{4}{\sqrt{\pi}}\left[1-b\,\lambda\,(1-\beta)\right]\left(\frac{\theta^{2.2}-\theta^{1/2}}{1-\theta^{0.55}}\right)\right\} \qquad (7)$$

To simplify the analysis, the cylindrical sample is assumed to be long compared to its radius such that axial flow can be neglected. If the sample is equilibrated at pressure p_A and then the pressure is removed at reduced time θ_d, the subsequent strain relaxation is given by

$$\varepsilon_z = (\varepsilon_\infty - \varepsilon_0)\,\Omega(\theta-\theta_d)\,. \qquad (8)$$

During depressurization, the sample experiences a tensile stress equal to the change in external pressure, so the jump in p_A must be smaller than the tensile strength of the sample. Alternatively, if higher pressures are required to get measurable strains, the measurement should only be made during pressurization; the pressure should tehn be released over a period of time comparable to the retardation time, τ_v (which was observed during retardation after the initial pressurization).

3. EXPERIMENTAL

3.1 Materials

Both hardened cement paste and concrete were tested using the DP technique. Cement pastes were chosen that matched those tested using the BB technique [15]. Pastes with *w/c* of 0.4, 0.5, and 0.6 were tested. The same cement used in the BB experiments, a Type III, was also used in this study. To test the potential for DP to be used for a practical test for concretes, a 0.50 *w/c* concrete was also tested. The mixture design for the concrete is shown in Table 1.

Table 1 – Mixture design for 0.50 *w/c* concrete

Constituent	Type	kg/m^3	lbs/yd^3
Cement	*Type III*	386	650
Course Agg.	*Crushed limestone*	977	1644
Fine Agg.	*Natural sand*	743	1250
Water	*~23° C*	193	325

3.2 Procedure and apparatus

The specimen geometry included 76 x 152 mm cylinders for the cement pastes, and 98 x 203 mm cylinders for the concrete. A 120 ohm 3-wire strain gage with a 50 mm gage length designed for embedment in cementitious materials was mounted axially in the center of the paste cylinder molds. The wire type gages had a diameter of 4 mm, and a dumbbell shape to ensure bond between gage and paste. An embedment strain gage with a dimpled polymeric casing surrounding a foil type inner gage element was mounted axially in the concrete cylinder molds. The concrete embedment gages were 3-wire with 350 ohm resistance. Both the 120 and 350 ohm gages were measured using a quarter bridge circuit.

The hydrostatic pressure was applied using an electric hydraulic pump and hydraulic oil, and controlled using an inline pressure regulator. The pressure was measured using an inline pressure sensor with an accuracy of 0.25%, and the pressure and strain data were recorded using an automated data collection system. The DP apparatus is illustrated in Fig. 1.

The cement pastes were mixed in a Hobart mixer according to ASTM C 305-99. After mixing, the pastes were cast into the cylinder molds in four equally sized lifts. After each lift, the cylinder mold was placed in a sealed container, vacuumed, then tapped for about 30 s to encourage the removal of entrapped air. The importance of removing entrapped air was stressed in the companion paper, and will be discussed in later in this paper.

The concrete was mixed in a pan style mixer. The water was added first to the fine and coarse aggregate and mixed for 30 s. The cement was then added and mixed for an additional 2 min. For a period of about 30 s, the pan bottom and sides were scraped. Finally, the material was mixed for an additional minute. The molds were filled with concrete using the same vacuuming procedure as with the pastes.

Specimens were demolded at an age of 12-18 hr, and then placed in a vacuumed vessel containing room temperature water with a lime addition of 0.2% to prevent leaching. Specimens were maintained in the vessel until the time of testing.

The test procedure involved placing the cement paste or concrete cylinders into a sealed pressure chamber filled. The pressure chamber was filled with saturated lime water up to the top surface of the cylindrical specimen, above which the chamber was filled with hydraulic oil (so that interference with the electrical strain measurement would be avoided). The desired pressure was set using an inline regulator and then a valve was opened to allow a ‘dynamic pressurization’ of the specimen. Pressure was ramped over a period of less than 1 s such that a step function pressurization could be used, simplifying the analysis. The pressure was held constant during the test. A constant temperature of 23° C was maintained by placing the pressure vessel in a thermal bath.

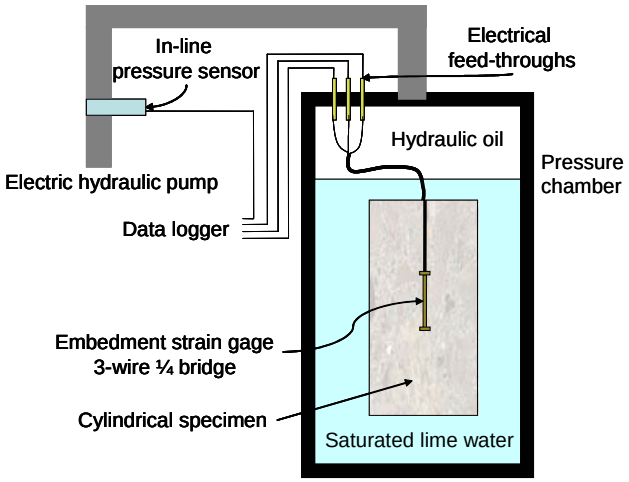

Fig. 1 – Apparatus for dynamic pressurization experiment.

4. RESULTS AND DISCUSSION

4.1 Permeability

Parameters required for determination of the permeability, k, from the DP test include the fluid properties K_L and η_L, the geometry R, the specimen properties υ_p, K_p, K_s, and ϕ, and the retardation time τ_v. If the temperature and fluid are known, then the fluid properties are also known. The geometry is controlled, and υ_p, K_p, and ϕ may be estimated since changes in these values have relatively little impact on the calculated k (see Eq. (5)). The parameter K_s is determined from the final strain after pressurization according to Eq. (3). Therefore, the parameter τ_v may be determined by fitting the retardation response to Eq. (7). The *expected* pressurization/depressurization response is shown graphically in Fig. 3 in the companion paper. For comparison, the typical *measured* retardation response on pressurization is shown in

Fig. 2 fitted to Eq. (8). Note that the compressive strain is plotted as positive.

Right side of the page
reserved to our referees

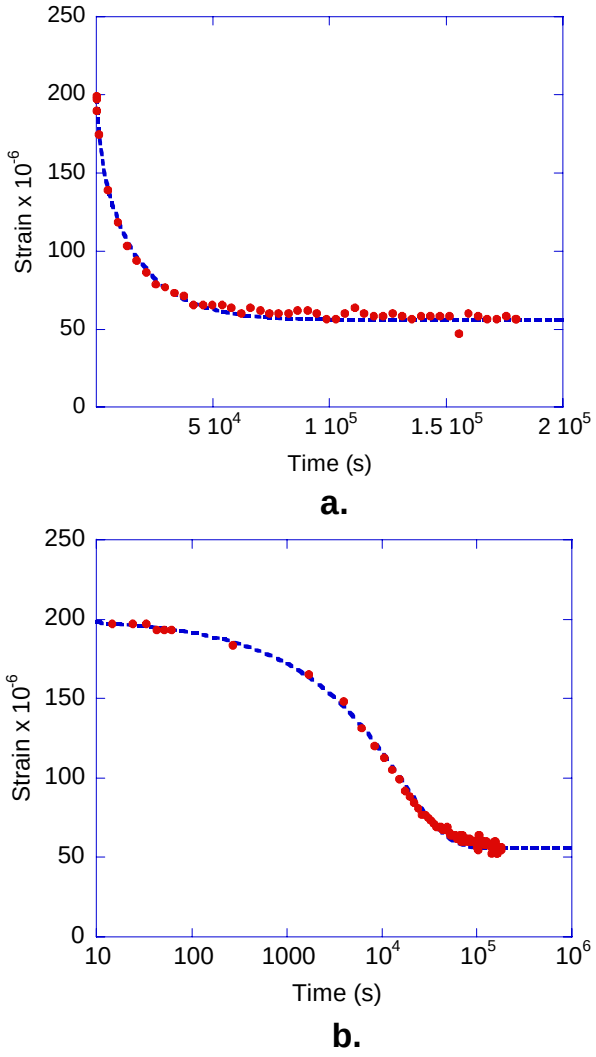

Fig. 2 – Typical retardation response fitted to Eq. (8). Compressive strain shown positive and on normal time (a.) and log time (b.) axes. Specimen is a 0.50 w/c paste subjected to 6.9 MPa hydrostatic pressure.

In specimens with little or no entrapped air, the DP test is quite repeatable. Fig. 3 illustrates the repeatability in two ways. First, on a mature specimen (minimal aging), subsequent pressurization-depressurization from the same hydrostatic pressure results in nearly identical retardation responses. Second, the repeatability between different samples is shown to be adequate at ages as early as 3 d.

As demonstrated in the companion paper, the presence of entrapped air greatly complicates the analysis. The pressure wave is slowed as it approaches the center of the specimen, and it is difficult to extract meaningful values for τ_v and K_s. Fig. 4 shows the deformation response of an unsaturated cylinder. The cylinder is a 0.5 w/c Type III cement paste for which no effort was made to eliminate entrapped air during mixing and casting. At an age of 24 hr, the specimen was placed under 2.1 MPa hydrostatic pressure, and axial strain

was measured. Note that the deformation is continuing over a period of several days, rather than hours. Also note the inflection in the curve caused by the compression of the air pockets. This inflection was predicted analytically in the companion paper (see Figure 8). The effect of *entrained* air has yet to be studied.

Another issue encountered when using the DP experiment is the potential for damage to occur. When an external hydrostatic pressure is applied, the solid skeleton is in a state of compression. Relatively high pressures may safely be used without the risk of damage. However, when a high external pressure is rapidly removed after the internal pore pressure has reached equilibrium, a condition is created where the center of the specimen has a significant hydrostatic pore fluid pressure while there is no external restraint. This places the solid skeleton under high tensile stress. If this stress exceeds the strength of the material, microcracking may result. The result of this microcracking is a higher apparent permeability on both the depressurization curve and on subsequent pressurization-depressurization cycles. Fig. 5 shows the pressurization and depressurization curves for a mature 0.6 *w/c* Type III cement paste exposed to 10.3 MPa external pressure. Notice that the rate of re-expansion after pressurization is much slower than the rate of contraction after the removal of the external pressure. Also, notice that the measured initial strain after pressure removal is significantly higher than the initial strain at the time of pressurization. While high pressures may be attractive from the standpoint that larger strains are measured, therefore improving resolution, the use of such pressures requires that the depressurization be performed in steps. Each pressure removal step must be less than the tensile strength of the material, and must be held long enough such that equilibrium occurs between the internal pore fluid and external pressures.

The expected pressurization-depressurization curves shown in Fig. 3 of the companion paper suggest that the final strain after depressurization should return to the zero strain prior to the application of hydrostatic pressure. This is typically true for mature materials, but for young, hydrating material, the final strain may not be zero. If an external pressure is applied for several hours to a hydrating material, at the time of pressurization the solid skeleton goes into compression. However, the formation of new hydration products must take place in a stress-free state. Just prior to pressure release, most of the solid skeleton is under compression, but a portion is stress free. After pressure release, the newly formed hydration products are under tension, and prevent the full return to zero strain. It has also been suggested that placing cement paste under a state of stress for long durations may increase the rate of reaction [23], exacerbating this issue. Any damage to the material due to high pressures may also result in a non-zero final strain.

When care is taken to avoid both damage and entrapped air, the DP test is both repeatable and accurate. Fig. 6 plots the measured permeability of both cement pastes and concretes using the DP test versus the measured permeability of identical materials using the BB technique. For the DP test, K_p values were assumed to be the same as those in the BB

test. Fig. 6 shows that there is excellent agreement between the BB results and the DP permeability results. It is clear that the permeability of the materials tested decreases with age until about 28 d, after which the value is relatively constant. There are a few data points for the 0.6 *w/c* paste that appears to indicate an increase in permeability after 30 d. This apparent increase is due to the damage effect described above.

The permeability values shown in Fig. 6 are expressed in units of length squared. This is the intrinsic permeability of the cementitious material, independent of fluid properties. Permeability of concrete is often expressed as *water permeability* in units of length/time, which is dependent on the fluid properties (viscosity, density). Intrinsic permeability, k, may be converted to water permeability, k_w, as

$$k_w = \frac{\rho g}{\eta_w} k \qquad (9)$$

where ρ is the density of water, g is the acceleration due to gravity, and η_L is the viscosity of water [24].

Right side of the page
reserved to our referees

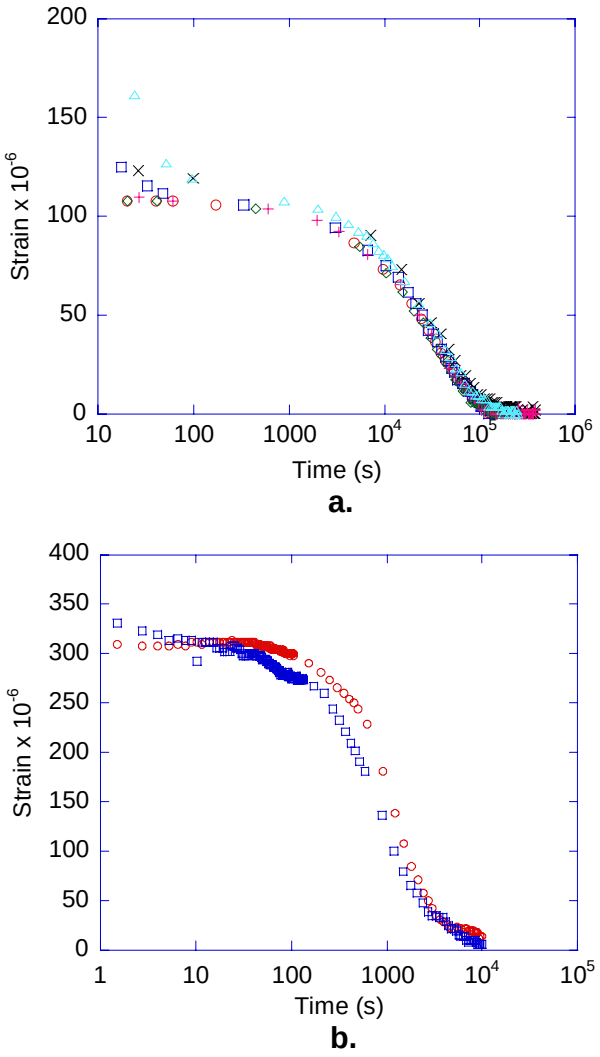

Fig. 3 – Demonstration of the repeatability of the DP experiment. a. Retardation curves of a mature 0.50 *w/c* paste specimen from two different pressurization and two different depressurization curves. b. Retardation curves of two 0.50 *w/c* paste specimens, 3 d age. Final strains zeroed to facilitate comparison.

Right side of the page
reserved to our referees

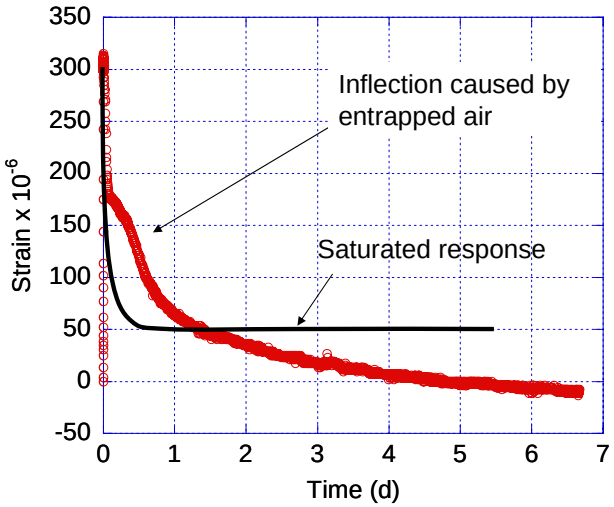

Fig. 4 – Effect of entrapped air on the retardation response of 0.50 w/c paste specimen. Note the inflection that is predicted analytically in the companion paper.

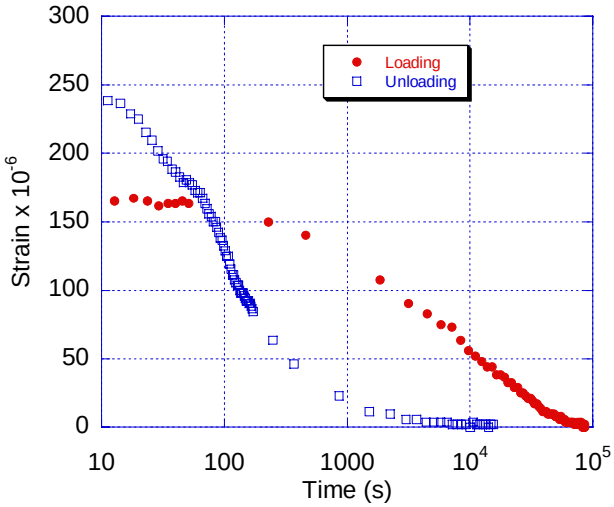

Fig. 5 – Effect of damage on the measured retardation response. Data shown is for first pressurizing then depressurizing from 10.3 MPa. Note the higher initial strain and more rapid re-expansion on depressurization. Final strain zeroed and both tensile and compressive strain shown as positive to facilitate comparison.

Right side of the page
reserved to our referees

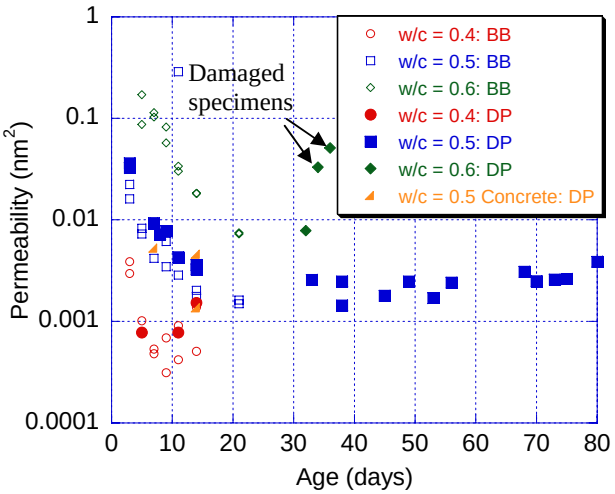

Fig. 6 – Comparison of dynamic pressurization (DP) permeability results with results obtained through beam bending (BB) experiments. BB data from [15].

4.2 Bulk modulus

The material property K_s was determined from the measured strain in the specimen once the pressure in the porous network had equilibrated with the externally applied pressure. At this point, the solid material was under hydrostatic pressure, and the strain remained relatively constant with time. The property K_s should be interpreted as the average bulk modulus of the material into which water cannot be intruded at the applied external pressure.

There are some important observations to be made in regard to the measured K_s for the cement pastes and concrete, which are listed in Table 2. First, K_s for the 0.50 w/c paste and concrete are very similar, in contrast to the significant difference expected between cement paste and concrete K_p. This implies that K_s for the paste is very similar to that of the aggregates. The aggregates used in this study have a Young's modulus of approximately 70 GPa, so if υ for the aggregate is assumed to be 0.2, the aggregate has a bulk modulus of about 39 GPa, which is in the same range as the measured K_s for the paste.

The second issue to recognize is that unlike K_p, K_s is relatively constant or decreasing at early age. A decrease with age (particularly at early age) is expected since hydration gradually converts cement particles to less dense hydration products. Clinker constituents C_3S and C_2S have reported Young's moduli of 125-160 GPa and Poisson ratio of 0.3 [25][25][26], which yields K_s of 104-133 GPa. Based on average Young's moduli reported for CH and C-S-H [27] and assumed average Poisson's ratio of 0.3, K_s for the hydration products range from 17-40 GPa, which is significantly lower than the clinker.

The overall magnitudes of the K_s values are reasonable considering that the solid nanostructure consists primarily of C-S-H and CH along with a portion of unhydrated C_2S and

C_3S.

The bulk modulus K_s as obtained in the DP experiment must be considered as a volumetric average value of the hydration products and any unhydrated cement grains. Theoretically, the solid nanostructure included in K_s may be dependent on the smallest pore diameter intruded by water at the testing temperature and applied pressure. However, according to Table 2, there is no systematic relationship between the applied pressure and the measured K_s.

Table 2 - Measured bulk modulus of the solid nanostructure, K_s.

0.50 w/c Paste			
Strain x 10^{-6}	Pressure (Mpa)	Age (d)	K_s (GPa)
16	2.5	7	53
39	4.4	9	38
47	6.9	14	49
63	6.9	17	36
0.40 w/c Paste			
Strain x 10^{-6}	Pressure (MPa)	Age (d)	K_s (GPa)
11	2.1	5	62
0.50 w/c Concrete			
Strain x 10^{-6}	Pressure (MPa)	Age (d)	K_s (GPa)
48	6.9	9	47.4
51	6.9	13	45.1

5. CONCLUSIONS

A new experimental method for measuring the permeability of a porous cementitious body and the bulk modulus of the solid nanostructure has been described. The analytical theory described by Scherer [20] has been validated through comparison to results obtained for identical materials using the beam bending method. The DP method allows rapid determination of water permeability (usually <24 hr test duration), and is repeatable. The permeability of cement paste and concrete have been measured as early as 3 d age. Since viscoelastic deformation is minimal, specimens may be retested at increasing ages to obtain the evolution of permeability with age. Standard sized cylinder molds may be used for casting specimens, making the method practical for concrete.

To ensure saturation at early ages the specimen must be vacuumed at mixing to eliminate entrapped air. Otherwise, many days may be required to obtain saturation, which is a necessary condition for extracting the bulk modulus and retardation time related to material permeability.

High pressures (greater than the tensile strength of the material) must be avoided in order to prevent damage to the specimen, which has been found to increase the apparent permeability of the specimen on subsequent testing.

The values of the bulk modulus of the solid nanostructure,

K_s, measured in the DP experiment compare well with values reported for the various individual phases obtained using nanoindentation techniques. The K_s measured with DP is an average value for the solid nanostructure, and is a useful parameter for modeling deformations caused by internal stresses such as drying shrinkage, autogenous shrinkage, and thermal dilation.

ACKNOWLEDGEMENTS

Zachary Grasley has been supported by an Eisenhower Fellowship through the National Highway Institute during this research. Experimental costs were supported by the Center of Excellence for Airport Technology (CEAT).

REFERENCES

[1] Hearn, N. and Mills, R.H., 'A simple permeameter for water or gas flow', *Cem. and Concr. Res.* **21 (**1991) 257-261.

[2] Sosoro, M., Hoff, W.D., and Wilson, M.A., 'Testing methods', in 'Penetration and Permeability of Concrete: Barriers to Organic and Contaminating Liquids', (E & FN Spon, London, 1997) 187-211.

[3] Banthia, N. and Mindess, S., 'Water permeability of cement paste', *Cem. and Concr. Res.* **19** (5) (1989) 727-736.

[4] Ye, G., 'The Microstructure and Permeability of Cementitious Materials', (Delft University Press, Delft, The Netherlands, 2003).

[5] El-Dieb, A.S. and Hooton, R.D., 'A high pressure triaxial cell with improved measurement sensitivity for saturated water permeability of high performance concrete', *Cem. and Concr. Res.* **24** (5) (1994) 854-862.

[6] Mehta, P.K. 'Pore size distribution and permeability of hardened cement paste', in '7th International Congress on the Chemistry of Cement', (Paris, 1980).

[7] El-Dieb, A.S., Hooton, R.D., 'Water-permeability measurement of high performance concrete using a high-pressure triaxial cell,' *Cem. & Concr. Res.* **25** (6) (1995) 1199-1208.

[8] Sellevold, E.J. and Richards, C.W., 'Short-time creep transition for hardened cement paste', *J. Amer. Cer. Soc.* **55** (6) (1972) 284-9.

[9] Ai, H., Young, J.F., and Scherer, G.W., 'Thermal expansion kinetics: Method to measure permeability of cementitious materials: II, Application to hardened cement pastes', *J. Amer. Cer. Soc.* **84** (2) (2001) 385-391. Erratum, *J. Amer. Cer. Soc.* **87** (8) (2004) 1611.

[10] Scherer, G.W., 'Thermal expansion kinetics: method to measure permeability of cementitious materials. I. Theory', *J. Amer. Cer. Soc.* **83** (11) (2000) 2753-61. Erratum, *J. Amer. Cer. Soc.* **87** (8) (2004) 1609-1610.

[11] Scherer, G.W., 'Thermal expansion kinetics - Method to measure permeability of cementitious materials: III, effect of viscoelasticity', *J. Amer. Cer. Soc.* **87** (8) (2004) 1509-1516.

[12] Scherer, G.W., 'Measuring permeability of rigid materials by a beam-bending method: I, Theory', *J. Amer. Cer. Soc.* **83** (9) (2000) 2231-2239. Erratum, *J. Amer. Cer. Soc.* **87** (8) (2004) 1615.

[13] Vichit-Vadakan, W. and Scherer, G.W., 'Measuring permeability and stress relaxation of young cement paste by beam bending', *Cem. and Concr. Res.* **33** (12) (2003) 1925-1932.

Right side of the page
reserved to our referees

[14] Valenza II, J. and Scherer, G.W., 'Measuring permeability of rigid materials by a beam-bending method: V, isotropic rectangular plates of cement paste', *J. Amer. Cer. Soc.* **87** (10) (2004) 1927-1931.

[15] Vichit-Vadakan, W., Scherer, G.W., and Grutzeek, M., 'Measuring permeability of rigid materials by a beam-bending method: III, cement paste', J *J. Amer. Cer. Soc.* **85** (6) (2002) 1537-1544.

[16] Grasley, Z.C., Lange, D.A., D'Ambrosia, M.D., 'Drying stresses and internal relative humidity in concrete', in 'Materials Science of Concrete VII', (American Ceramic Society, 2005).

[17] Bissonette, B., Marchand, J., Charron, J.P., Delagrave, A., Barcelo, L., 'Early age behavior of cement-based materials', in 'Materials Science of Concrete VII', (American Ceramic Society, 2001).

[18] Bentz, D.P., Garboczi, E.J. and Quenard, D.A., 'Modelling drying shrinkage in reconstructed porous materials: application to porous Vycor glass', *Mod. and Simul. in Mat. Sci. and Eng.* **6** (3) (1998) 211-36.

[19] Lura, P., Guang, Y.E., van Bruegel, K., 'Effect of cement type on autoegenous deformation of cement-based materials', *ACI* **SP 220-4 (**2004) 57-68.

[20] Scherer, G.W. 'Dynamic pressurization method for measuring permeability and modulus: I. Theory', *Mat. & Struct.* submitted (2005).

[21] Gross, J. and Scherer, G.W., 'Dynamic pressurization: Novel method for measuring fluid permeability', *J. of Non-Cryst. Sol.* **325** (1-3) (2003) 34-47.

[22] Biot, M.A., 'General theory of three-dimensional consolidation', *J. of App. Phys.* **12** (2) (1941) 155-164.

[23] Tamtsia, B.T., Beaudoin, J.J. and Marchand, J., 'The early age short-term creep of hardening cement paste: Load-induced hydration effects', *Cem. and Concr. Comp.* **26** (5) (2004) 481-489.

[24] Muskat, M., 'The Flow of Homogenous Fluids Through Porous Media', (McGraw-Hill, New York, 1937).

[25] Velez, K., Maximilien, S., Damidot, D., Fantozzi, G., and Sorrentino, F., 'Determination by nanoindentation of elastic modulus and hardness of pure constituents of portland cement clinker', *Cem. and Concr. Res.* **31** (4) (2001) 555-561.

[26] Acker, P. 'Micromechanical analysis of creep and shrinkage mechanisms', in 'ConCreep 6', Proceedings of an International Conference, Massachusetts Institute of Technology, 2001 (Elsevier, 2001).

[27] Constantinides, G. and Ulm, F.-J., 'The effect of two types of C-S-H on the elasticity of cement-based materials: Results from nanoindentation and micromechanical modeling', *Cem. and Concr. Res.* **34** (1) (2004) 67-80.